AIAA 80-1002R

Acoustic Pressures on a Prop-Fan Aircraft Fuselage Surface

B. Magliozzi*
United Technologies, Windsor Locks, Conn.

Acoustic pressure amplitude and phase distributions on the surface of a simulated fuselage (a rigid semicylinder) installed in an acoustically treated wind tunnel near a prop-fan model were measured. The test conditions simulated the relative tip Mach number and blade loading of a full-scale prop-fan at high altitude 0.8 Mach number cruise. Measurements were also made at equivalent microphone locations without the semicylinder to establish the effects of the presence of a fuselage on the sound pressure amplitudes. These effects were found to be 6 dB at 90 deg incidence, decreasing to no effect at grazing incidence. Comparison of measurements and calculations using a Hamilton Standard prop-fan noise calculation computer program showed good agreement in peak level and in phase distribution. Continuous recordings were also made of a prop-fan rpm sweep at constant simulated flight speed and a simulated flight speed sweep at constant prop-fan rpm. These showed smooth variations in noise level over the tip Mach number range 0.878-1.143.

Introduction

ADVANCED turboprop propulsion is currently being investigated as a means of improving fuel efficiency of future transport aircraft. Initial studies as summarized in Ref. 1 have shown that the advanced turboprop (prop-fan) is more fuel efficient than advanced high-bypass-ratio turbofans. The objectives for a prop-fan powered airplane are to provide increased efficiency at 0.7-0.8 Mach number cruise with cabin noise levels similar to those of current turbofan transports.

Initial studies have indicated that sufficiently high levels of exterior noise will exist owing to the prop-fan so that interior noise levels would exceed current objectives, assuming fuselage noise reduction values of contemporary airframe structure. Although the fuselage noise reduction can be increased, current technology methods result in increased fuselage weight. However, these approaches do not address the discrete low-frequency noise spectrum of the prop-fan propulsion concept. By incorporating a specific noise reduction goal into the fuselage structural design process, the effectiveness of the structure in reducing noise can be significantly improved over that of a conventional structure of the same weight.[2] Thus, although extra weight will be required in the structure of a prop-fan powered airplane, it can be minimized by incorporating the noise reduction goals in the fuselage design.

In order to design an advanced fuselage, the noise reduction requirements must first be established. This is dependent on the exterior noise field, which must be defined in terms of amplitude and (owing to the discrete nature of prop-fan noise) phase distributions on the fuselage surface. The exterior noise field can be calculated using available noise prediction methodology. Although measurements of prop-fan noise exist,[3-5] prop-fan noise levels incident on a fuselage surface under cruise conditions were not available for verification of the predictions. Thus an experimental program to acquire this information was undertaken.

This paper presents the results of such a measurement program, in which the noise incident on a rigid model fuselage was measured under simulated cruise in model scale. Comparisons of measurements and calculations were also made. Finally, predictions of noise amplitude and phase contours on the surface of a full-scale airplane fuselage in high speed cruise were made.

Presented as Paper 80-1002 at the AIAA 6th Aeroacoustics Conference, Hartford, Conn., June 4-6, 1980; submitted July 24, 1980; revision received March 30, 1981.

*Senior Analytical Engineer, Hamilton Standard Division.

Test Program

Model Description

The SR-3 prop-fan model was used for this test program. This model, shown in Fig. 1, is an eight-blade configuration with moderate blade sweep designed to operate at 800 ft/s tip speed at 0.8 Mach number cruise at 35,000 ft altitude. A discussion of the aeroacoustic design of the model can be found in Ref. 6. This 2-ft-diam model was installed on an aerodynamically clean drive rig. Although designed to operate in an eight-blade configuration, the model was tested in a four-blade configuration to accommodate the drive motor power limitation. In this configuration, the design power loading per blade of an eight-blade configuration could be achieved.

For this test program a simulated fuselage model was constructed from ¼-in.-thick steel boiler plate. As a 30-in.-diameter half cylinder, it provides a prop-fan-to-fuselage diameter ratio similar to that for a full-scale airplane. The fuselage model was used for testing at two tip clearances which have been proposed for full-scale airplanes. For 0.4 prop-fan diameter tip clearance testing, the fuselage model was attached to the inlet nozzle so that the surface was immersed in boundary layer flow, simulating a fuselage in flight. Figure 2 shows the four-bladed prop-fan model and the simulated fuselage at a tip clearance of 0.4 prop-fan diameter.

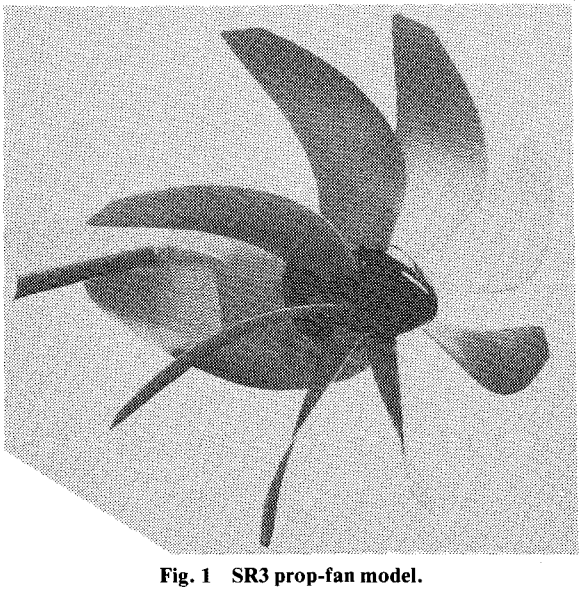

Fig. 1 SR3 prop-fan model.

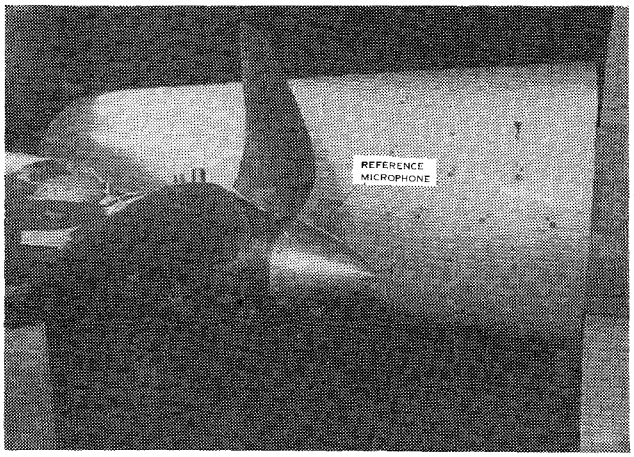

Fig. 2 Simulated fuselage acoustic test setup.

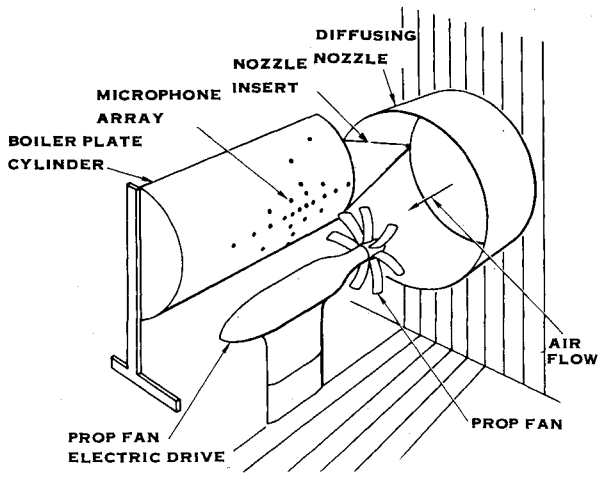

Fig. 3 Prop-fan, nozzle, and fuselage model arrangement.

For 0.8 prop-fan diameter tip-clearance testing, the fuselage was detached from the nozzle and located outside the tunnel flow stream.

Facility Description

All testing for this program was conducted in the Acoustic Research Tunnel at the United Technologies Research Center (UTRC) in East Hartford, Connecticut. A detailed description of this facility is given in Ref. 7. The tunnel is an open-circuit, open-jet design (Eiffel configuration). The test chamber is lined with fiberglass wedges to provide an anechoic acoustic environment over a frequency range of 200 to 20 kHz. A detailed discussion of the tunnel setup for prop-fan model acoustic testing is given in Ref. 3.

A 46-in.-diam nozzle with a three-dimensional insert was used. The insert was used to fair the flow from the concave nozzle to the convex fuselage. Figure 3 shows the nozzle-fuselage-prop-fan model arrangement. With this arrangement, the prop-fan model is immersed in the potential core of the jet. Within the boundary layer flow region on the fuselage, the cruise flight flowfield was simulated. Hot-wire anemometry and flow visualization confirmed that the prop-fan model was well within the low turbulence flow of the tunnel jet potential core and that the simulated fuselage was within a well-defined turbulent boundary layer at all but the outermost microphone locations.

Measurement System

The noise incident on the model fuselage was measured using Bruel & Kjaer (B&K) ⅛-in. condenser microphones. The microphone outputs were recorded on magnetic tape for later analysis. The B&K microphones were selected because of their low phase distortion (from about 3 deg phase lag at 10 kHz to about 10 deg at 20 kHz). The microphones were flush-mounted on the fuselage surface using vibration isolation mounting plugs.

Six channels of acoustic data were recorded during each test run. In order to minimize channel-to-channel phase distortion, the acoustic data signals were recorded using a single seven-channel record head on the tape recorder. For correlation of acoustic data with rotor position and to obtain harmonic order analyses, a reference signal from a once-per-revolution (1P) photoelectric pulse generator (pipper) located on the prop-fan drive shaft was recorded on the remaining channel.

Test Procedure

The acoustic test configuration for the simulated fuselage located in the tunnel flowfield (tip clearance of 0.4 prop-fan diameter) is shown in Fig. 4. Since the outputs of only six microphones were recorded in one pass, all microphone

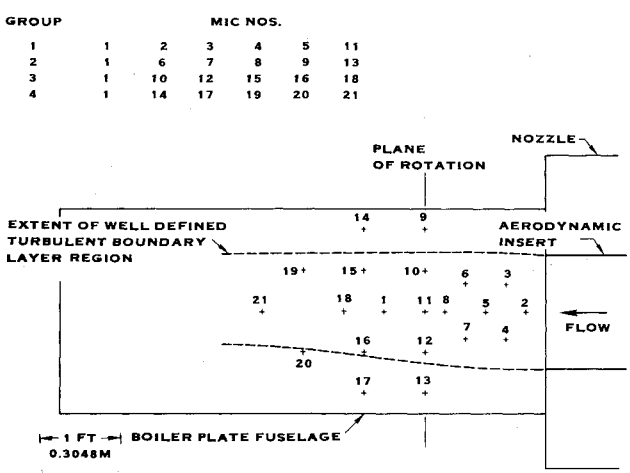

Fig. 4 Boiler plate fuselage microphone identification and location.

positions were recorded in four groups of six microphones as indicated in the figure. The No. 1 microphone was kept fixed and was recorded with each group as a reference. The remaining five microphones were moved to different locations for each test run.

A summary of the test conditions is given in Table 1. A test condition map is shown in Fig. 5. Measurements were made at three rotational speeds: 9000, 10,000, and 11,300 rpm. The 9000 rpm testing was done with a tunnel Mach number of 0.20, while a nominal tunnel Mach number of 0.265 was used for the remaining testing. Since the tunnel was operated below the full-scale prop-fan cruise Mach number, the model was oversped to achieve full-scale design relative tip speeds. However, a blade loading distribution, which approximates that in cruise, was retained. The three test rpm's corresponded approximately to relative tip Mach numbers of 0.91 (subsonic), 1.02 (transonic), and 1.15 (supersonic). Similar tests were run with the fuselage moved out of the tunnel flowfield to a tip clearance of 0.8 prop-fan diameters. In addition, as indicated by the lines in Fig. 5, limited data were taken for slow, continuous sweeps of both prop-fan rpm and tunnel Mach number. The rotational speed was swept from 8500-11,300 rpm at a constant tunnel Mach number of about 0.266. The tunnel Mach number was swept from 0.188 to 0.289 for constant 10,000 rpm prop-fan speed.

Also, data were taken at 13 free-field locations corresponding to selected fuselage locations at the 0.8-diam tip-clearance position, using two microphone arrays. This was done to establish the effects of the fuselage on measured noise (reflecting surface effects).

Data Reduction

All the acoustic data were analyzed using a narrow-band frequency analyzer. The analysis range used was 0-20 kHz, which gave an effective filter bandwidth of 60 Hz. From these analyses, the harmonic sound pressure levels were determined at each of the microphone locations. Since the data were acquired using a four-bladed prop-fan, only every other harmonic (8P multiples) was used to simulate the spectrum of an eight-bladed prop-fan. Adding 6 dB (for doubling the number of blades) to each 8P harmonic would then exactly simulate the noise that would be produced by an eight-bladed prop-fan.

Since the data from the 21 microphone locations on the fuselage were acquired in four passes, the data from three passes were adjusted to conditions equivalent to those of the fourth pass. The data adjustment was made on the basis of the measurements made using the fuselage reference microphone and the free-field reference microphone, which were both common to the four passes.

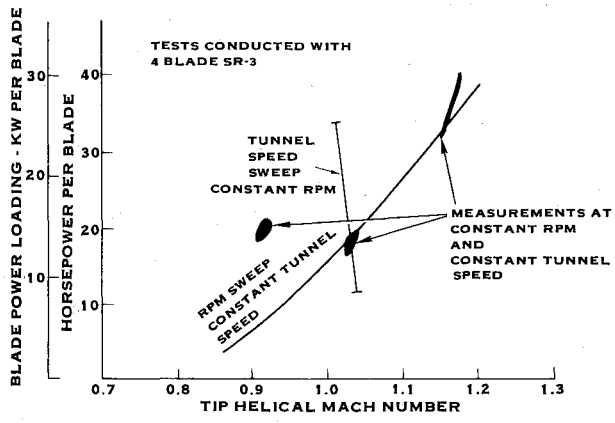

Fig. 5 Simulated fuselage acoustic test operating conditions.

Because the absolute phase of the acoustic signal is of no consequence, only the relative phase distributions on the simulated fuselage were desired. Therefore the relative phases and amplitudes of the acoustic signals were determined by doing a transfer function analysis on the data, using the fuselage reference microphone signal as the input signal and each of the other microphone signals as the output signals. The transfer function, $H(f)$, was calculated from the cross-power spectrum from

$$H(f) = \frac{S_y(f)}{S_x(f)} = \frac{S_y(f)}{S_x(f)} \frac{S_x^*(f)}{S_x^*(f)} = \frac{G_{xy}(f)}{G_{xx}(f)}$$

where $S_x(f)$ and $S_y(f)$ are the Fourier transforms of inputs x and y, $G_{xy}(f)$ is the cross-power spectrum of x and y, $G_{xx}(f)$ is the power spectral density (PSD) of x, and * denotes complex conjugate. In this analysis, x was always the fuselage reference microphone and y was each of the other microphones.

Since $H(f)$ is a complex quantity, it can be represented by a magnitude and a phase. The magnitude of $H(f)$ represents the amplitude of the signal relative to that of the reference signal (P_y/P_{ref}) while the phase of $H(f)$ represents the phase difference ($\theta_y - \theta_{ref}$). Only the phase difference was used; and, since θ_{ref} is common to all the data, the quantity ($\theta_y - \theta_{ref}$) defines the relative phase distribution on the fuselage.

Table 1 Summary of boilerplate fuselage test operating conditions

Run no.	Blade angle, deg	Temperature K	Temperature °F	Tunnel Mach no.	rpm	Power kW	Power hp	Tip helical Mach no.	Comments
263	21.5	304	88	0.267	11,300	94.3	126.4	1.143	Fuselage at
264		305	89	0.267	10,000	48.2	64.6	1.016	0.4 diam tip
265		304	88	0.201	9,000	52.3	70.1	0.901	clearance
266		298	76	0.267	11,300	100.2	134.3	1.155	
267		297	75	0.267	10,000	55.5	74.4	1.028	
268		297	75	0.200	9,000	58.3	78.2	0.911	
269		299	79	0.265	11,300	101.4	135.9	1.151	
270		299	78	0.265	10,000	51.8	69.5	1.025	
271		299	78	0.200	9,000	56.9	76.3	0.909	
272		299	79	0.267	11,300	100.2	134.3	1.152	
273		299	79	0.265	10,000	50.8	68.1	1.024	
274		299	78	0.200	9,000	57.9	77.6	0.909	
277	21.5	295	71	0.268	11,300	104.9	140.6	1.160	3 microphones in
278		294	69	0.270	10,000	53.9	72.3	1.035	potential core
279		293	68	0.201	9,000	61.1	81.9	0.917	
280	21.5	291	64	0.267	11,300	120.1	161.0	1.167	Fuselage at
281		291	64	0.266	10,000	58.1	77.8	1.038	0.8 diam tip
282		292	65	0.201	9,000	62.1	83.2	0.920	clearance
285		297	75	0.266	11,300	109.5	146.8	1.156	
286		297	75	0.266	10,000	58.6	78.5	1.028	
287		297	75	0.200	9,000	62.1	83.2	0.911	
288		299	78	0.266	11,300	105.5	141.4	1.153	
289		301	82	0.266	10,000	54.5	73.0	1.022	
290		301	81	0.199	9,000	62.5	83.8	0.906	
291		301	81	0.269	11,300	105.5	141.4	1.151	
292		301	81	0.269	10,000	51.8	69.5	1.023	
293		302	84	0.204	9,000	55.1	73.8	0.905	
294	21.5	301	82	0.268	11,300	108.4	145.3	1.149	No fuselage
295		302	83	0.269	10,000	52.9	70.9	1.022	equivalent free-
296		301	82	0.202	9,000	57.9	77.6	0.906	field locations
297		300	80	0.269	11,300	107.8	144.5	1.152	at 0.8 diam tip
298		299	79	0.269	10,000	50.3	67.4	1.025	clearance
299		299	79	0.200	9,000	56.9	76.3	0.908	

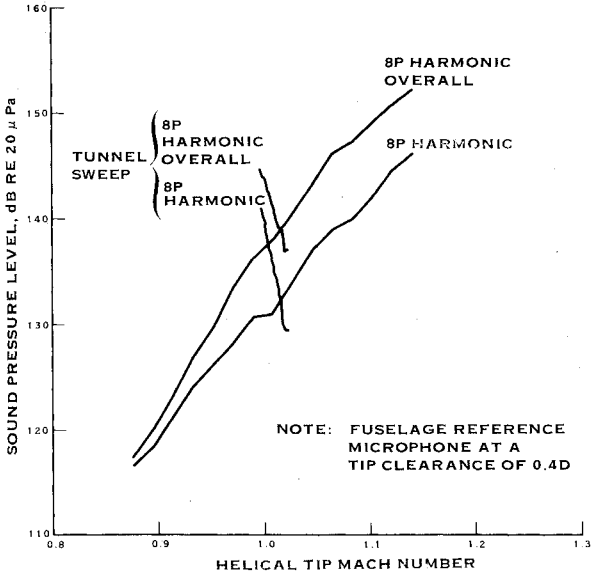

Fig. 6 Variation of prop-fan noise level with tip Mach number.

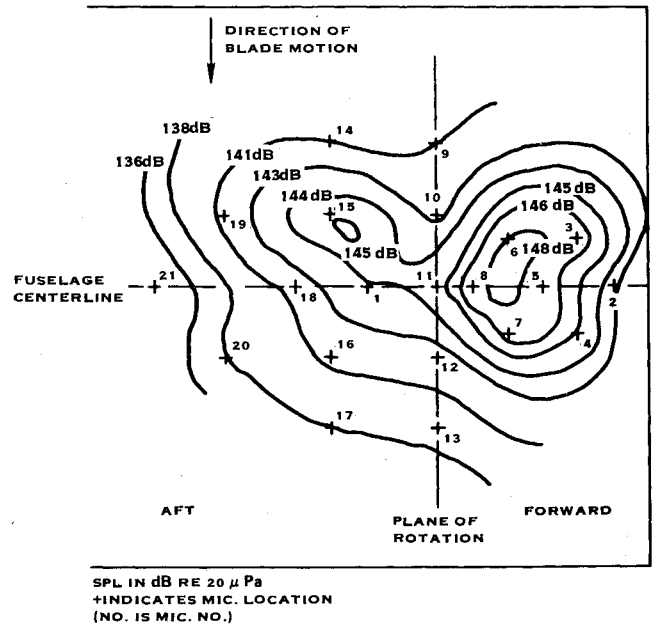

Fig. 7 Measured sound pressure amplitude contours at 11,300 rpm for the 4P harmonic.

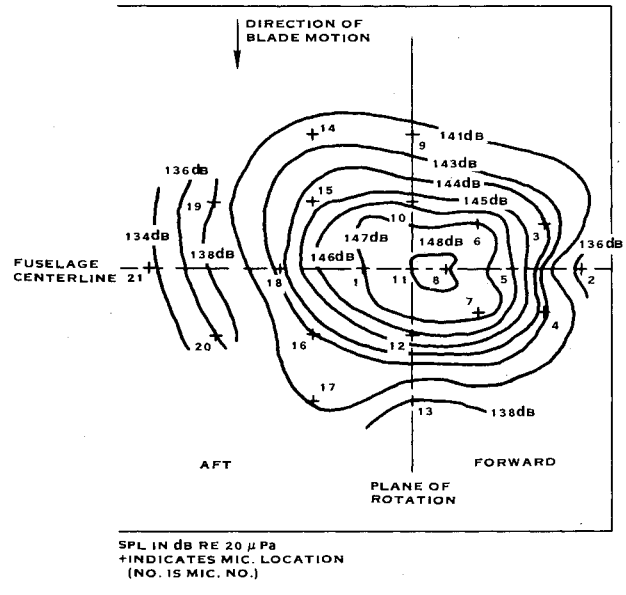

Fig. 8 Measured sound pressure amplitude contours at 11,300 rpm for the 8P harmonic.

The transfer function was calculated digitally. The data were first digitized synchronously using the 1P pipper as a clock input to avoid smearing and aliasing. The 1P pipper was multiplied by 102.4 so that each time frame of 1024 points would contain exactly ten cycles of the acoustic signal. A 512-point Fourier transform was then done on each time frame, with 120 transforms averaged for each analysis. Since the data were highly periodic, only those points in the transforms corresponding exactly to blade passing frequency harmonics had any significance. The rest was random noise. Thus only every 40th point in the transform was used. Because of the synchronous sampling and integral time frames used, these corresponded exactly to the blade passage frequency harmonics.

Phase calibration was accomplished by playing back the phase calibration data (simultaneous injection of pure tones to the microphone preamplifier) through the same playback/data reduction system. This provided relative phases between the reference microphone channel and each of the other data channels as functions of frequency. The microphone phase distortion was assumed negligible so that the only phase distortion correction applied to the data was that of the record/playback system determined as described above.

Experimental Results

rpm and Tunnel Mach Number Sweep

The sound pressure level variation with prop-fan relative tip Mach number is summarized in Fig. 6. The rpm sweep data show a fairly smooth noise level increase from a relative tip Mach number of 0.878 (8500 rpm) to a relative tip Mach number of 1.143 (11,300 rpm). The overall level based on 8 P harmonics (i.e., using every other harmonic from the measurements to simulate an eight-bladed prop-fan) increases more rapidly than does the 8P fundamental because the rise in the higher harmonics is greater than that in the lower harmonics. It should be noted that the rapid increase in noise is due to an increase in power input (from 20 hp at 8500 rpm to 133 hp at 11,300 rpm) as well as an increase in tip speed.

The tunnel Mach number sweep at 10,000 rpm also shows a smooth noise level variation with tip Mach number. In this case, however, the increasing tunnel speed results in an unloading of the prop-fan (from 135 hp at low tunnel speed to 45 hp at high tunnel speed). Apparently, the blade loading effect on noise is stronger than that of tip Mach number.

It can thus be concluded that the variation in prop-fan noise level with tip Mach number is a smooth function with no discontinuities in the transonic region. As these measurements were made with a flush mounted microphone located on the simulated fuselage in the tunnel flow, it is then apparent that the noise from a full-scale prop-fan incident on an airplane fuselage will not exhibit unusually intense high-frequency components as found in tests of supersonic tip speed propellers conducted in the 1950's.

Harmonic Amplitude Contour Plots

The harmonic levels, determined from the narrow-band frequency analyses, were used to define constant sound pressure amplitude contours on the model fuselage. Figures 7 and 8 show the measured contours for the first two harmonics of blade passing frequency for the 11,300 rpm condition with the simulated fuselage at 0.4 prop-fan diameter clearance. A maximum level of about 148 dB was measured for the fundamental (4P) and is seen in Fig. 7 to occur slightly ahead of the plane of rotation. A second local peak occurs at a level of

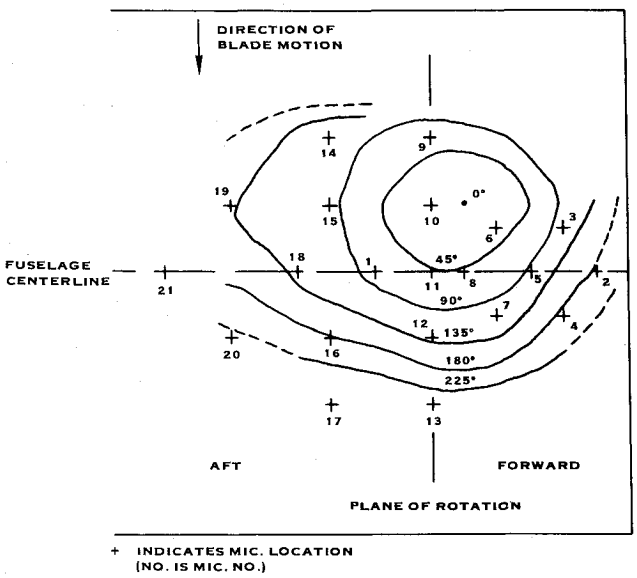

Fig. 9 Measured sound pressure phase angle contours at 11,300 rpm for the 4P harmonic.

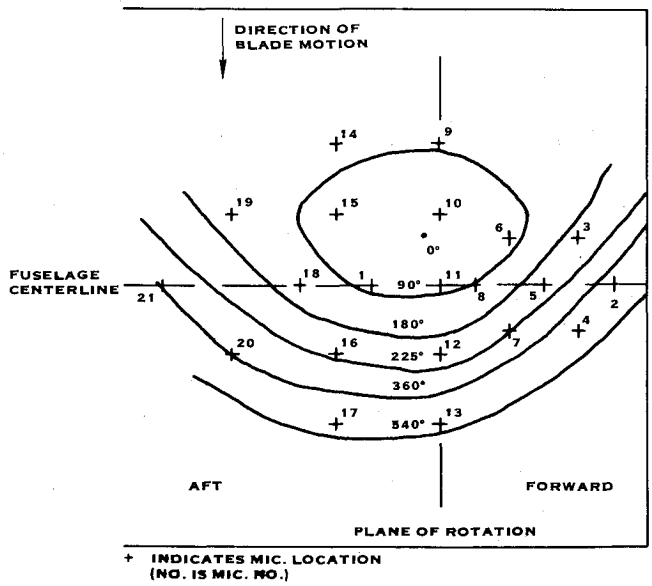

Fig. 10 Measured sound pressure phase angle contours at 11,300 rpm for the 8P harmonic.

Table 2 Derived reflection effects based on measured fuselage and free-field prop-fan noise levels (fuselage at 0.8 diam clearance)

Microphone no.	9000 rpm average, dB	10,000 rpm average, dB	11,300 rpm average, dB	Total average, dB	Incidence angle, deg
1	5.05	7.65	5.00	5.9	70.6
2	−1.80	6.60	3.50	2.8	46.3
3					57.3
4					38.3
5	−5.35	−0.75	−9.20	−5.1	54.9
6					68.2
7					43.1
8	5.80	8.70	6.00	6.8	63.3
9	10.00	7.95	5.90	8.0	45.2
10	4.05	8.00	7.40	6.5	74.0
11	7.30	6.90	4.50	6.2	66.8
12	5.60	7.85	5.45	6.3	36.9
13	1.05	2.40	2.10	1.9	10.3
14					43.4
15	5.40	8.15	7.85	7.1	73.8
16	4.85	5.80	2.70	4.5	39.4
17					12.3
18	8.20	6.00	6.40	6.9	69.1
19					64.8
20					40.3
21	−2.90	2.25	5.05	1.5	59.8

about 145 dB behind the plane of rotation. The contours are seen to be unsymmetrical about the fuselage centerline. This occurs, in part, because of the unsymmetrical reflection effects due to the curved fuselage surface. Figure 8 shows the contours for the second harmonic (8P), which has its peak noise level occurring just ahead of the plane of rotation. It may be noted that the contours are more closely spaced below the fuselage centerline than above the centerline. This occurs because the acoustic wave incidence is closer to normal on the top surface, while the wave incidence on the lower surface approaches grazing.

Harmonic Phase Angle Contour Plots

Measured phase angle contour plots are shown in Figs. 9 and 10 for the 4P and 8P harmonic, respectively. These contours are nearly elliptical and are centered on a point slightly ahead of the plane of rotation and above the fuselage centerline. As would be expected, owing to the shorter wavelength for the 8P harmonic, these contours show a more rapid change in phase than those for the 4P harmonic.

Reflecting Surface Effects

The effects of the fuselage as a reflecting surface were determined by comparing the levels measured with the fuselage at the 0.8 prop-fan diameter location with those measured at the equivalent free-field location. The data showed essentially no dependence on frequency, as generally expected, since the wavelengths are short enough relative to the fuselage diameter to be in the realm of geometric acoustics. In order to help remove some of the scatter, the data for ten harmonics of blade passing frequency for the three rpm's were averaged. Table 2 summarizes the average reflection effects and the calculated sound incidence angles. The sound incidence angles were calculated considering convection and shear-layer transmission effects, as described in detail in Ref. 8.

The reflection effects (i.e., levels measured on the fuselage minus those measured in free-field) are shown plotted against incidence angle in Fig. 11. Although there is considerable scatter in these data, the cluster of points beyond 60 deg incidence angle suggests that a pressure doubling effect of 6 dB

was attained. The data between 30 and 60 deg show three points less than 6 dB and only two points above 6 dB, suggesting that the reflection effects are decreasing with decreasing incidence angle. This is supported by the point at 10.3 deg.

Although the substantial amount of scatter (not surprising since the total anticipated effect is only 0-6 dB) prevents identification of a clear trend in reflection effects with incidence angle, pressure doubling (6 dB) at normal incidence decreasing to no effect at a grazing incidence is suggested. The somewhat arbitrary exponential curve fit passing through 0 dB at 0 deg and 6 dB at 60 deg shown in Fig. 11 is suggested by the data and used later in this report for reflection corrections as functions of incidence angle.

Comparison of Measured and Calculated Prop-Fan Noise

Sound Pressure Amplitudes

4P and 8P harmonic noise levels on the simulated fuselage surface located at 0.4 prop-fan diameter clearance for the prop-fan operating at the 11,300 rpm condition were calculated using the current Hamilton Standard prop-fan noise prediction methodology. As this procedure calculates noise under free-field conditions, the empirically derived reflecting surface effects were added to the estimates for comparison with the levels measured on the simulated fuselage.

The calculated 4P harmonic amplitude contours are shown in Fig. 12 compared to those measured. The peak level of 148 dB is well predicted, although the secondary peak seen in the measurements is not predicted. This secondary peak is due to loading noise, which was not well calculated by the prop-fan noise prediction methodology available at the time of the test for the low-through-flow velocities at the Acoustic Research Tunnel conditions (a detailed discussion of comparisons of measured and calculated model prop-fan noise is given in Ref. 3). The agreement is fairly good on the forward, lower quadrant of the fuselage, with contour shapes and levels being in agreement. In the other three quadrants, the noise levels are generally overpredicted. Thus, in general, the calculated contours are more closely spaced along the fuselage centerline and extend further along the upper fuselage surface than do the measured levels. Thus the calculated surface areas enclosed by the contours match the measurements fairly well, although the shapes are somewhat distorted.

Figure 13 shows the comparison between calculated and measured 8P harmonic amplitude contours. Both the peak value of 148 dB and the location of the 148-dB "island" are well predicted. Again, the agreement is quite good in the forward, lower quadrant. Although the agreement is not as good in the other three quadrants, it is better than that obtained for the 4P harmonic. For this harmonic the areas enclosed by the contours are in excellent agreement.

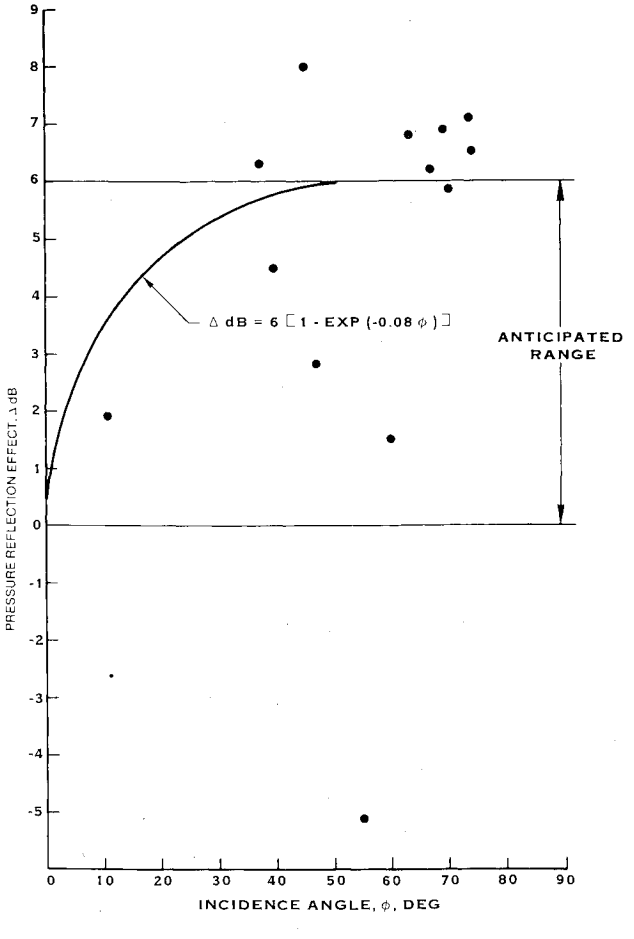

Fig. 11 Dependence of the reflection effect on incidence angle.

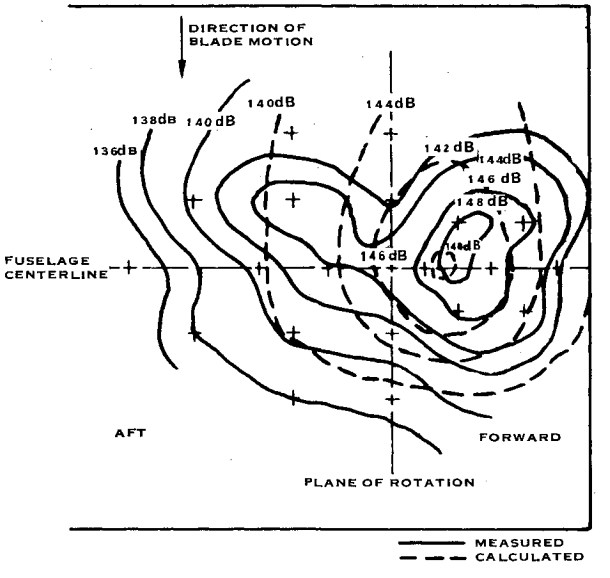

Fig. 12 Comparison of measured and calculated sound pressure amplitude contours at 11,300 rpm for the 4P harmonic.

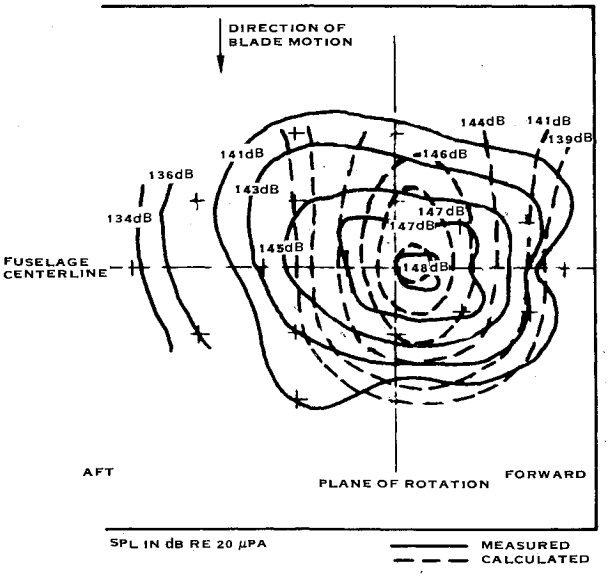

Fig. 13 Comparison of measured and calculated sound pressure amplitude contours at 11,300 rpm for the 8P harmonic.

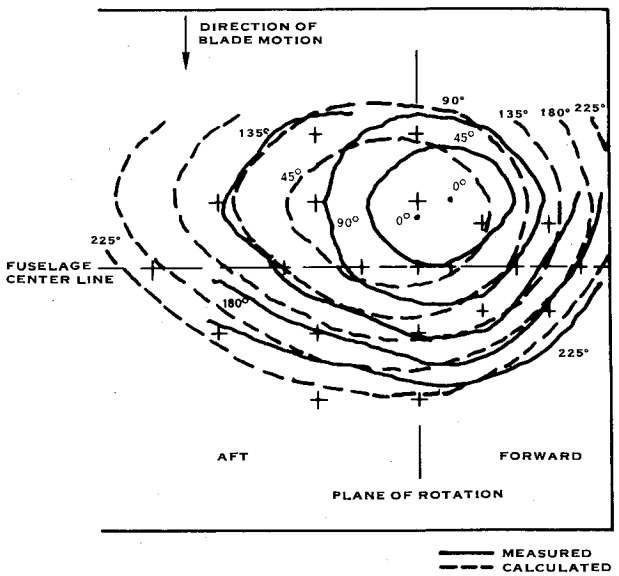

Fig. 14 Comparison of measured and calculated sound pressure phase angle contours at 11,300 rpm for the 4P harmonic.

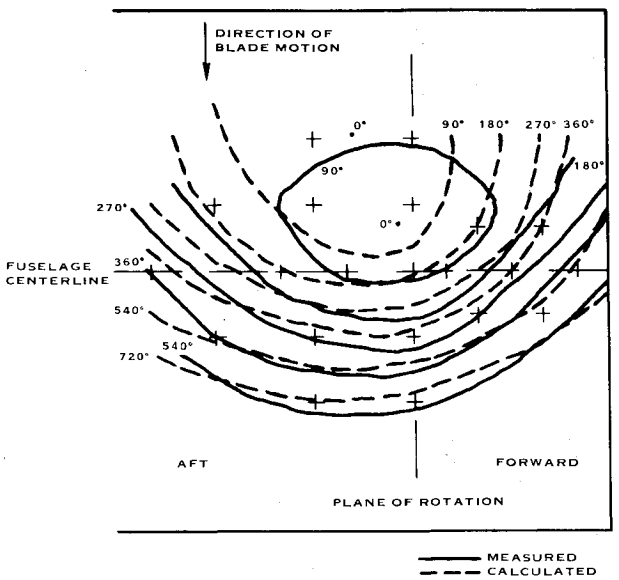

Fig. 15 Comparison of measured and calculated sound pressure phase angle contours at 11,300 rpm for the 8P harmonic.

Sound Pressure Phases

The calculated phase angle contours for the 4P harmonic are shown compared to the measured contours in Fig. 14. As may be seen, the agreement is fairly good. The rate of change of the phase for the calculations along the plane of rotation and behind the plane of rotation is in close agreement with that measured. Forward of the plane of rotation, the calculations show a less rapid change than that shown by the measurements.

Figure 15 shows the comparison for the 8P harmonic. Although the location of the 0-deg phase point is not well calculated, the rate of phase change in the range 180-720 deg is well calculated.

Although the calculations show contours which are ellipse-like with a vertical major axis whereas the measurements show a horizontal major axis, the enclosed areas are in excellent agreement. Thus, based on these comparisons, it is believed that the calculations of amplitude and phase contours for the full-scale prop-fan at cruise conditions will be representative of the actual contours. This is supported by the discussion of Ref. 3, which indicates that the noise can be more accurately calculated for the actual cruise conditions than for the model test conditions.

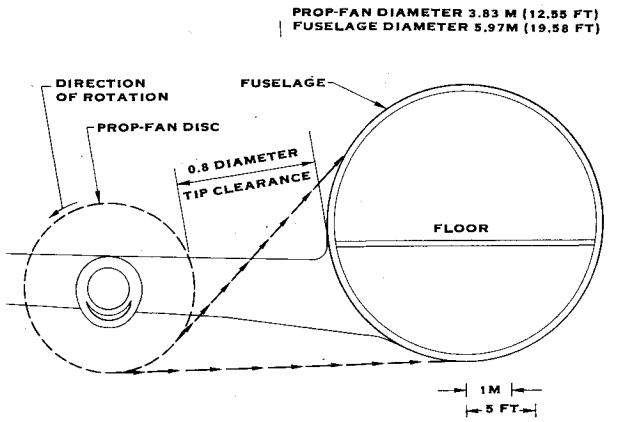

Fig. 16 Full-scale front view of aircraft configuration used for fuselage surface pressure predictions.

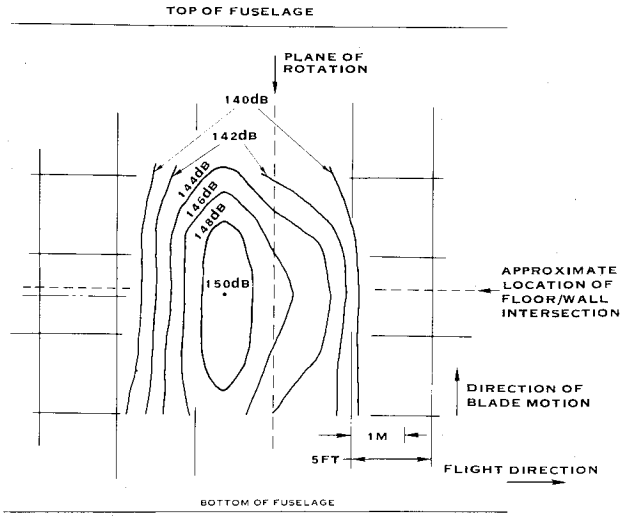

Fig. 17 Unwrapped view of sound pressure amplitude contours at blade passage frequency predicted for full-scale prop-fan airplane.

Full-Scale Predictions

Configuration

Sound pressure level and phase angle contours were estimated for a full-scale prop-fan operating at cruise conditions. For these estimates, a 12.55-ft-diam prop-fan with eight SR-3-type blades operating at a tip speed of 800 ft/s with a power input of 5900 hp was assumed for a 35,000-ft-altitude cruise at 0.8 Mach number. The geometry for the installation is summarized in Fig. 16.

Sound Pressure Level Contours

The sound pressure level contours were estimated on the basis of free-field noise estimates at the fuselage locations. These were adjusted for fuselage reflection effects, using the adjustments based on angle of incidence from Fig. 11. The angle of incidence was calculated from the geometry shown in Fig. 16, assuming a cylindrical fuselage and apparent source location due to convection effects.

Figure 17 presents the predicted sound pressure level contours for the fundamental blade passing frequency tone. A peak noise level of 150 dB (including reflection effects) is estimated. Owing to convection effects, the peak noise level

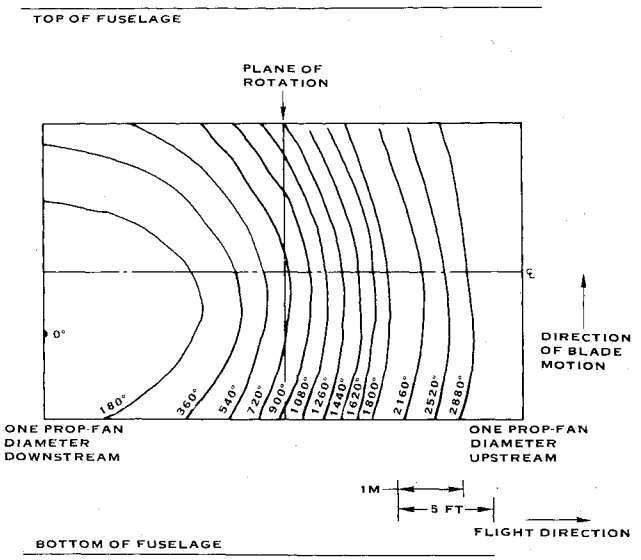

Fig. 18 Unwrapped view of sound pressure phase angle contours at blade passage frequency predicted for full-scale prop-fan airplane.

appears behind the plane of rotation. At the peak noise level location, the reflection effect is +6 dB. The 10-dB down points are about 5 ft behind the peak noise level location and 8.5 ft ahead of the peak noise level location. It may also be seen that the sound pressure level contours closely follow the fuselage circumference behind the peak noise location. Ahead of the peak noise level location, the contours are expanded, primarily owing to reduced reflection effects caused by shallower incidence angles. The contours are also contracted near the top of the fuselage owing to reduced reflection effects as the incidence angles are near grazing in this area.

Phase Angle Contours

Figure 18 shows the calculated phase angle contours for the fundamental blade passing frequency tone. The phase angles are predicted to change slowly from the zero-phase point to the 180-deg phase contour. Beyond the 180-deg phase contour, the phase changes very rapidly, increasing from a 180-deg change in a distance of 2 ft at a location 3 ft behind the plane of rotation to a change of 360 deg in a distance of 1 ft at a location 9 ft ahead of the plane of rotation.

Conclusions

Measurements of noise from a prop-fan with moderate blade sweep incident on a model fuselage immersed in tunnel flow simulating flight conditions indicate a smooth rise in level with increasing tip relative Mach number with no rapid increase in level through the transonic region. It is thus expected that full-scale prop-fan noise incident on an airplane fuselage in cruise will be more acceptable than that experienced in the 1950's with unswept propellers operating at supersonic tip speeds.

The major effect of a fuselage located in proximity to a prop-fan is to cause an increase in the amplitude of the incident noise. The increase is due to reflection effects and is dependent on angle of incidence. It varies from no effect at grazing incidence to 6 dB for incidence angles greater than 60 deg.

Comparison of predicted model prop-fan noise levels on the simulated fuselage, using the current Hamilton Standard noise prediction methodology and the empirically derived reflection effects, showed excellent agreement with the measured levels at the peak noise location. The calculated contours were somewhat more closely spaced along the centerline and extended further along the upper surface than those measured.

A full-scale version of the early (SR3) prop-fan design tested in this program, in an eight-bladed configuration at 0.8 Mach number cruise located at 0.8-diam tip clearance, is estimated to produce a peak noise level of 150 dB, including reflection effects, at the blade passing frequency. The 10-dB down points are estimated to be 5 ft behind the peak noise location and 8.5 ft ahead of the peak noise location.

Acknowledgment

This work was supported by the NASA Lewis Research Center under Contract NAS3-20614.

References

[1] Dugan, J.F., Gatzen, B.S., and Adamson, W.M., "Prop-Fan Propulsion—Its Status and Potential," SAE Paper No. 780995, Nov. 1978.

[2] Bhat, R.B., Sobieszczinski, J., and Mixson, J.S., "Reduction of Aircraft Cabin Noise by Fuselage Structural Optimization," *Proceedings of the National Noise and Vibration Control Conference and Exhibition,* NOISEXPO '77, March 1977, pp. 40-45.

[3] Brooks, B.M and Metzger, F.B., "Acoustic Test and Analysis of Three Advanced Turboprop Models," NASA CR159667, Jan. 1980.

[4] Dittmar, J.H., Blaha, B.J., and Jeracki, R.J., "Tone Noise of Three Supersonic Helical Tip Speed Propellers in a Wind Tunnel at 0.8 Mach Number," NASA TM79046, Dec. 1978.

[5] Dittmar, J.H., Jeracki, R.J., and Blaha, B.J., "Tone Noise of Three Supersonic Helical Tip Speed Propellers in a Wind Tunnel," NASA TM79167, June 1979.

[6] Metzger, F.B. and Rohrbach, C., "Aeroacoustic Design of the Prop-Fan," AIAA Paper No. 79-0610, March 1979.

[7] Paterson, R.W., Vogt, P.G., and Foley, W.M., "Design and Development of the United Aircraft Research Laboratories Acoustic Research Tunnel," *Journal of Aircraft,* Vol. 10, No. 7, 1973, pp. 427-433.

[8] Magliozzi, B. and Brooks, B.M., "Advanced Turbo-Prop Airplane Interior Noise Reduction—Source Definition," NASA CR159668, Oct. 1979.